

First Ferromagnetic Interaction in a Heteropoly Complex: $[\text{Co}^{\text{II}}_4\text{O}_{14}(\text{H}_2\text{O})_2(\text{PW}_9\text{O}_{27})_2]^{10-}$. Experiment and Theory for Intramolecular Anisotropic Exchange Involving the Four Co(II) Atoms[†]

Nieves Casañ-Pastor,[†] Julia Bas-Serra,[§] Eugenio Coronado,[§] Genevieve Pourroy,[‡] and Louis C. W. Baker*

Contribution from the Department of Chemistry, Georgetown University, Washington, D.C. 20057, and the Department of Inorganic Chemistry, University of Valencia, 46100-Valencia, Spain. Received August 3, 1992

Abstract: The four coplanar Co(II) atoms in $\text{K}_{10}[\text{Co}_4\text{O}_{14}(\text{H}_2\text{O})_2(\text{PW}_9\text{O}_{27})_2] \cdot 22\text{H}_2\text{O}$ occupy the vertices of a rhomb in a Co_4O_{16} entity. Each Co atom is somewhat off-center in its edge-sharing CoO_6 octahedron. The corrected effective magnetic moment is essentially constant at $\sim 10.4 \mu_B$ down to 40 K, corresponding to four independent Co(II) atoms each having spin = $3/2$ and significant spin-orbit coupling. Below 20 K the complex exhibits strong ferromagnetic coupling, μ_{eff} rising to over $14.4 \mu_B$ and the Curie-Weiss θ becoming $\sim +6$ K. Below 9 K μ_{eff} tends toward leveling out again, in accordance with the isolated nature of the intramolecular ferromagnetic coupling in the heteropoly system. This is the first report of ferromagnetic coupling in a heteropoly complex and apparently the first case of a polynuclear Co(II) system showing intramolecular ferromagnetic exchange. Furthermore, the complex provides a novel geometrical arrangement of the four edge-sharing CoO_6 octahedra, which increases interest in the explanation of the magnetic interaction. The results emphasize the potential value of heteropoly complexes for magnetic studies because of the magnetic isolation of the groups of interacting atoms and the existence of isomorphous series of complexes containing a wide variety of combinations of paramagnetic atoms. Owing to the combined effects of spin-orbit coupling and distortion, each octahedral Co(II) atom behaves below ~ 30 K as an anisotropic spin doublet, $S = 1/2$, as confirmed by the low-temperature ESR spectrum of the complex doped into the diamagnetic isomorph wherein Zn replaces Co. The two structural types of Co require different g tensors. Evaluation of the exchange and Zeeman Hamiltonians leads to a best fit to the data below 22 K requiring $2J_{\parallel} = +19 \text{ cm}^{-1}$, $J_{\perp}/J_{\parallel} = 0.321$, $g_{\parallel} = 7.9$ and 6.15 , and $g_{\perp} = 2.04$ and 5.1 . Emphasis is placed on the necessity for anisotropy if the data are to fit, more than on the specific values of the parameters. The magnetic results and the structure lead to suggestion of an explanation of the ferromagnetism involving some overlap of magnetic orbitals of adjacent Co's and the orbital degeneracy of the Co, thereby allowing electronic transfers in their t_{2g} orbitals, which keep a parallel spin alignment on the virtual Co(III)-Co(I) excited state, thus providing a pathway for stabilization of the ferromagnetic state. Work on isomorphs is in progress aimed at elucidating this point.

This is the first report of ferromagnetic coupling in a heteropoly complex and thus points to systems that potentially have several advantages for study of high-spin molecules, an area of strongly emerging interest.¹ To our knowledge this is also the first report of a discrete ferromagnetic complex based on the magnetically interesting element Co.^{2,3}

Heteropoly complexes^{4,5} resemble discrete fragments of mixed metal oxide structures of definite sizes and shapes. They maintain their identities in aqueous and nonaqueous solutions and in ionic crystals. Many heteropoly complexes can be made which contain diverse combinations of d-transition metal atoms at specific sites.⁴⁻¹¹ Sizeable varieties of bond angles, coordination geometries, oxidation states, and linkages between numerous paramagnetic atoms are available in pure complexes. Because the groups of paramagnetic atoms are generally isolated in the individual heteropoly complexes, complications from intermolecular (lattice) interactions are negligible.¹¹ These compounds also offer numerous combinations of paramagnetic atoms in various series of isomorphous complexes. The isomorphism obviates major complications in comparative interaction studies. These factors are well-illustrated by the present complex, for which isomorphous salts exist^{6,7} wherein the Co(II) atoms in the magnetically isolated Co_4O_{16} group in each complex are replaced by atoms of another transition metal or by combinations of atoms of such metals.

In the past our group exploited the above-cited characteristics of heteropoly complexes to elucidate, experimentally and theoretically, a different isomorphous series that exhibits complete antiferromagnetic coupling of spins at low temperatures, approaches complete decoupling at high temperatures, and has a large intermediate temperature range (> 150 °C) in which susceptibility changes very little.^{8,11} Examples of antiferromagnetic interaction among three V(IV) atoms and among three Cu(II) atoms in heteropoly complexes have been elucidated.^{10b,12} We have recently carried out an extensive study of interactions between delocalized "blue" electrons in heteropoly frameworks and para-

(1) (a) Papers presented at Symposium on "Molecular Ferromagnets and High Spin Molecules"; 197th National Meeting of the American Chemical Society, Dallas, 1989. *Mol. Cryst. Liq. Cryst.* **1989**, *176*. (b) Bino, A.; Johnston, D. C.; Goshorn, D. P.; Halbert, T. R.; Stiefel, E. I. *Science* **1988**, *241*, 1479.

(2) Cairns, C. J.; Busch, D. H. *Coord. Chem. Rev.* **1986**, *69*, 1.

(3) Ferromagnetic coupling between Co(II) atoms has been found in the infinite linear chain compound CoTAC: Groenendijk, H. A.; Van Duyneveldt, A. J. *Physica* **1982**, *115B*, 41.

(4) (a) Baker, L. C. W. In *Advances in the Chemistry of the Coordination Compounds*; Kirschner, S., Ed.; Macmillan: New York, 1961; pp 608ff. (b) Evans, H. T. *Perspect. Struct. Chem.* **1971**, *4*, 1. (c) Weakley, T. J. R. *Struct. Bonding (Berlin)* **1974**, *18*, 131.

(5) Pope, M. T. *Heteropoly and Isopoly Oxometalates*; Springer-Verlag: Berlin, 1983.

(6) Weakley, T. J. R. et al. *J. Chem. Soc., Chem. Commun.* **1973**, 139.

(7) Evans, H. T.; Tourné, C. M.; Tourné, G. T.; Weakley, T. J. R. *J. Chem. Soc., Dalton* **1986**, 2699.

(8) Baker, L. C. W., et al. *J. Am. Chem. Soc.* **1966**, *88*, 2329.

(9) Baker, L. C. W.; Figgis, J. S. *J. Am. Chem. Soc.* **1970**, *92*, 3794.

(10) For example: (a) Finke, R. G.; Drooge, M. W. *Inorg. Chem.* **1983**, *22*, 1006. (b) Kokoszka, G. F.; Padula, F.; Goldstein, A. S.; Venturini, E. L.; Azevedo, L.; Siedle, A. R. *Inorg. Chem.* **1988**, *27*, 59.

(11) Baker, L. C. W.; Baker, V. E. S.; Wasfi, S. H.; Candela, G. A.; Kahn, A. H. *J. Am. Chem. Soc.* **1972**, *94*, 5499; *J. Chem. Phys.* **1972**, *56*, 4917.

(12) Mossoba, M. M.; O'Connor, C. J.; Pope, M. T.; Sinn, E.; Hervé, G.; Težé, A. *J. Am. Chem. Soc.* **1980**, *102*, 6864.

[†]Original version submitted July 1989. Experimental data and partial theoretical rationalization abstracted from the Ph.D. Dissertation of N. Casañ-Pastor, Georgetown University, 1988.

[‡]Present address: Institute of Materials Science of Barcelona, CSIC, Campus UAB, 08193-Bellaterra, Barcelona, Spain.

[§]Permanent affiliation: Department of Inorganic Chemistry, Faculty of Sciences, University of Valencia, 46100-Valencia, Spain.

[‡]Dept. Science Matériaux, EHICS, 67008-Strasbourg, France.

* Address correspondence and reprint requests to this author at Georgetown University.

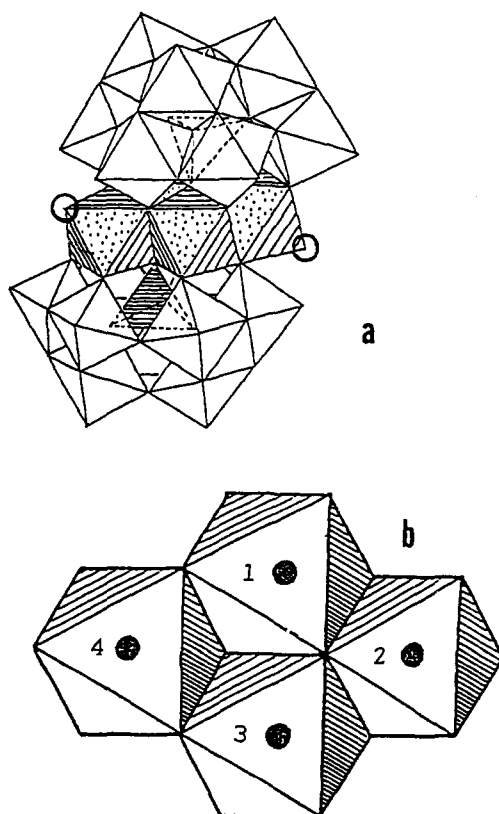


Figure 1. (a) The structure of the $[\text{Co}_4(\text{H}_2\text{O})_2(\text{PW}_9\text{O}_{34})_2]^{10-}$ complex.^{6,7} Each vertex of a polyhedron locates the center of an oxygen atom. Each white octahedron contains a W atom, displaced off-center toward its octahedron's unshared oxygen. Each tetrahedron contains a P atom. Each shaded octahedron contains a Co atom. The circles locate the O atoms of the H_2O molecules coordinated to two of the Co atoms. (b) Diagram of the Co_4O_{16} central group. The filled circles locate the four coplanar Co(II) ions.

magnetic heteroatoms in various sites.¹³ In addition to pertinence for magnetic studies, heteropoly complexes are proving especially valuable for elucidation of a number of interrelated areas of current interest including catalysis; intermolecular and intramolecular electron transfer;^{14,15} metal oxide conductivity,^{15,16} different types, mechanisms,^{5,18} and pathways^{13,16-22} for mixed-valence electron delocalization and for extensive d-electron spin delocalization;^{21,22} and theory of multinuclear NMR chemical shifts^{17,19,21-24} and electron spin couplings.^{11,14,16,17}

The present study focuses on the heteropoly anion $[\text{Co}^{\text{II}}_4\text{O}_{14}(\text{H}_2\text{O})_2(\text{PW}_9\text{O}_{27})_2]^{10-}$ first reported by Weakley et al.,⁶ the structure of which⁷ is shown in Figure 1. That complex contains a Co_4O_{16} group consisting of four coplanar $\text{Co}^{\text{II}}\text{O}_6$ octahedra sharing edges. Five of the Co-O-Co angles are 90° while each

(13) (a) Casañ-Pastor, N. Doctoral Dissertation, Georgetown University, 1988. (b) Casañ-Pastor, N.; Baker, L. C. W. *J. Am. Chem. Soc.*, following paper in this issue.

(14) Kozik, M.; Baker, L. C. W. *J. Am. Chem. Soc.* **1987**, *109*, 3159.

(15) Kozik, M.; Hammer, C. F.; Baker, L. C. W. *J. Am. Chem. Soc.* **1986**, *108*, 7627.

(16) Kozik, M.; Casañ-Pastor, N.; Hammer, C. F.; Baker, L. C. W. *J. Am. Chem. Soc.* **1988**, *110*, 7697.

(17) Kozik, M. Doctoral Dissertation, Georgetown University, 1987.

(18) Barrows, J. N.; Jameson, G. B.; Pope, M. T. *J. Am. Chem. Soc.* **1985**, *107*, 1771.

(19) Kozik, M.; Hammer, C. F.; Baker, L. C. W. *J. Am. Chem. Soc.* **1986**, *108*, 2748.

(20) Sanchez, C.; Livage, J.; Launay, J. P.; Fournier, M. *J. Am. Chem. Soc.* **1983**, *105*, 6817.

(21) Acerete, R.; Casañ-Pastor, N.; Bas-Serra, J.; Baker, L. C. W. *J. Am. Chem. Soc.* **1989**, *111*, 6049.

(22) Jorris, T. L.; Kozik, M.; Casañ-Pastor, N.; Domaille, P. J.; Finke, R. G.; Miller, W. K.; Baker, L. C. W. *J. Am. Chem. Soc.* **1987**, *109*, 7402.

(23) Acerete, R.; Hammer, C. F.; Baker, L. C. W. *J. Am. Chem. Soc.* **1982**, *104*, 5384.

(24) Acerete, R. Doctoral Dissertation, Georgetown University, 1981.

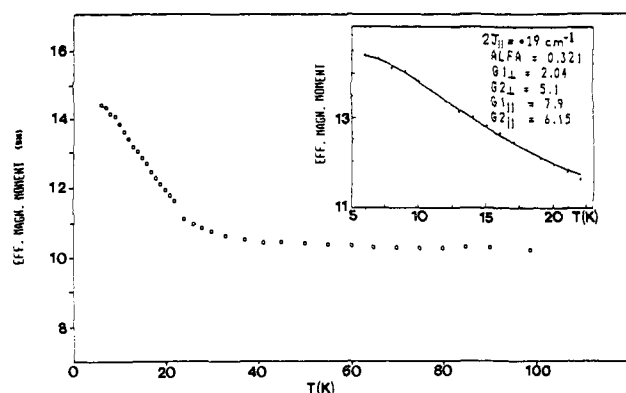


Figure 2. Plots of corrected μ_{eff} values versus T . Circles and crosses are experimental data. The insert is an expansion of the low-temperature portion. The line represents the best theoretical fit according to the model assumed.

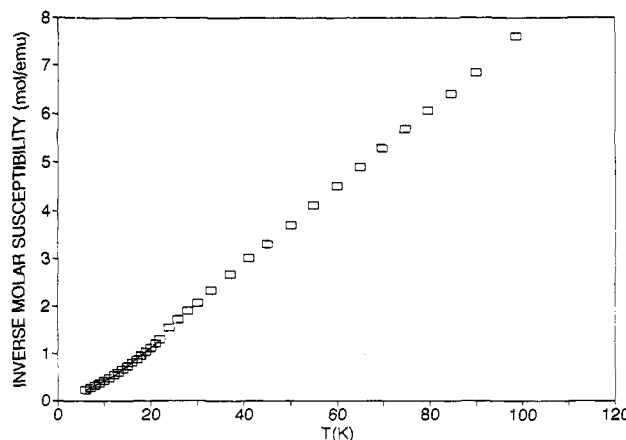


Figure 3. Plot of corrected inverse molar susceptibilities versus T (K). The solid line represents best-fit calculated values.

of the other five is $\sim 100^\circ$. That is, each CoO_6 octahedron is distorted because each of the four coplanar Co atoms is somewhat off-center in its octahedral site.

The results of the magnetic study are summarized by Figures 2 and 3, which show that μ_{eff} remains essentially constant at $\sim 10.4 \mu_B$ down to 40 K. That value corresponds to four independent Co(II) ions each having spin = $3/2$ and a significant spin-orbit coupling contribution. (The spin-only value is $7.74 \mu_B$.) The plot of inverse corrected molar susceptibilities versus T (Figure 3) shows that between 40 and 20 K the slope increases decidedly, reaching a Curie-Weiss θ of $\sim +6$ K, in accordance with intramolecular ferromagnetic exchange. Below 40 K μ_{eff} increases to over $14.4 \mu_B$. Below 9 K the curvature reverses so that μ_B tends toward leveling out again (Figure 2) and the $1/\chi$ vs T plot (Figure 3) tends toward eventual extrapolation to the origin.

Such behavior clearly demonstrates ferromagnetic exchange between Co atoms, with negligible interaction between Co_4O_{16} groups in neighboring heteropoly complexes. These results will be discussed in terms of an anisotropic exchange model. The unexpected sign of the exchange correlates with the structure of the Co_4O_{16} entity and with the orbital degeneracy of the Co(II) ions.

Experimental Section

Recrystallized $\text{K}_{10}[\text{Co}_4\text{O}_{14}(\text{H}_2\text{O})_2(\text{PW}_9\text{O}_{27})_2] \cdot 22\text{H}_2\text{O}$, prepared as described by Finke and Droege²⁵ and showing the same UV-vis spectrum,²⁵ was examined in a Model 905 variable temperature susceptometer equipped with a SQUID sensor (Biomagnetic Technologies, formerly SHE Corp.). The applied field was 5000 G, and the temperature range was 6–100 K. The Al-Si sample bucket was 0.75×0.45 cm. Diamagnetic correction was based on the value determined by Simmons²⁶

(25) Finke, R. G.; Droege, M. *J. Am. Chem. Soc.* **1981**, *103*, 1587.

Table I. Observed and Calculated Molar Susceptibilities (χ_m) for $K_{10}[\text{Co}_4\text{O}_{14}(\text{H}_2\text{O})_2(\text{PW}_9\text{O}_{27})_2]\cdot 22\text{H}_2\text{O}^a$

T (K)	exptl $\chi_{m,corr}$ (emu)	calcd χ_m (emu)
6.005	4.3237	4.3188
6.995	3.6726	3.6660
7.990	3.1283	3.1526
9.005	2.7447	2.7320
10.005	2.3908	2.3914
11.015	2.1030	2.1068
12.015	1.8644	1.8712
12.995	1.6637	1.6763
13.995	1.5142	1.5076
15.005	1.3696	1.3624
16.000	1.2513	1.2399
17.005	1.1376	1.1331
18.000	1.0444	1.0416
18.995	0.9614	0.9617
19.995	0.8914	0.8914
20.995	0.8265	0.8294
21.995	0.7677	0.7745
23.995	0.6444	
25.990	0.5789	
27.990	0.5260	
30.000	0.4818	
32.990	0.4279	
36.990	0.3733	
41.000	0.3310	
44.970	0.3024	
49.975	0.2703	
54.970	0.2437	
59.980	0.2224	
64.750	0.2040	
69.700	0.1890	
74.650	0.1760	
79.600	0.1647	
84.550	0.1561	
89.900	0.1462	
98.550	0.1314	

^a Calculated χ_m values evaluated using $\alpha = 0.321$, $2J_{\parallel} = +19 \text{ cm}^{-1}$, and best-fit g values quoted in the text and in Figure 2. Molecular weight = 5518; mass = 0.1178 g; applied field = 5000 G; diamagnetic correction = $-890 \times 10^{-6} \text{ emu/mol}$; TIP correction for octahedral Co(II) $\times 4$ Co atoms = $600 \times 10^{-6} \text{ emu/mol}$.

for $\text{K}_4[\text{SiW}_{12}\text{O}_{40}]\cdot 11\text{H}_2\text{O}$ ($\chi_m = -507 \times 10^{-6} \text{ emu/mol}$) appropriately modified by means of Pascal constants²⁷ to account for removal of Si and WO_6 units, addition of P and Co atoms, and change of hydration. Experimental molar susceptibility values corrected for diamagnetism and TIP are given in Table I. Each data point is an average of ten measurements taken over about a 1-h period after the temperature stabilized. The susceptibility values (and the magnetic moments) are subject to an estimated 2% maximum error, arising in large part because of minor uncertainty about the molecular weight, given the zeolitic nature of much of the water of hydration in efflorescent heteropoly salts. X-band ESR spectra at 4 K of the Co_4 complex doped into the potassium salt of the diamagnetic Zn_4 isomorph gave $g_1 = 7.0$, $g_2 = 3.9$, and $g_3 = 2.8$.

Discussion

Owing to the combined effect of spin-orbit coupling and distortion, octahedral Co(II) behaves at low enough temperature ($T < 30 \text{ K}$) as an anisotropic spin doublet, $S = 1/2$ (as indicated by the anisotropy shown by the ESR g values). Thus, an anisotropic exchange model is expected to be appropriate for analysis of the magnetic properties²⁸

$$H_{ex} = -2 \sum_{i < j} J_{ij\parallel} S_{iz} S_{jz} - 2 \sum_{i < j} J_{ij\perp} (S_{ix} S_{jx} + S_{iy} S_{jy}) \quad (1)$$

where \parallel and \perp refer to the components parallel and perpendicular to the spin direction, and i and j label the Co sites. In view of the symmetry of the rhomb-like Co_4O_{16} entity (Figure 1), four

Table II. Statistical Goodness of Fit Values (F) for Various Imposed α Values

$2J_{\parallel}$ (calcd), cm^{-1}	$\alpha = J_{\perp}/J_{\parallel}$	F
20.07	0.0 ^a	0.81
20.14	0.2	0.17
18.89	0.3	0.15
22.29	0.4	0.18
27.99	0.6	0.26
21.04	0.8	1.1

^a Ising model.

of the five nearest neighbor Co interactions must be identical ($J_{12} = J_{23} = J_{34} = J_{14}$, numbering the Co atoms as in Figure 1). Although by symmetry J_{13} must be somewhat different, it has been taken as equal to each of the foregoing. This reasonable assumption reduces the number of adjustable parameters in the fitting procedure and yields satisfactory results. Taking into account that the Co_4O_{16} groups contain two types of metal sites, two different g tensors are to be expected in the Zeeman Hamiltonian (below): g_a for sites 1 and 3 and g_b for sites 2 and 4.

The best fit to the data involves the following set of parameters: $2J_{\parallel} = +19 \pm 1 \text{ cm}^{-1}$, $J_{\perp}/J_{\parallel} = \alpha = 0.321$, $g_{\parallel a} = 7.9$, $g_{\parallel b} = 6.15$, $g_{\perp a} = 2.04$, $g_{\perp b} = 5.1$. The statistical goodness of fit, F , is similar for values of α between 0 and 0.4, although the best value is 0.321. See Table II, which also shows that the goodness of fit becomes rapidly worse when α values exceed 0.4 (i.e., become closer to isotropic exchange).

Emphasis is placed on the fact that anisotropy must be introduced in order for the data to fit, rather than on the specific value for the exchange anisotropy indicated. It is to be noted that the amount of anisotropy indicated by the foregoing calculation is comparable to that reported for cases of Co in other compounds.²⁸ Further, it is in agreement with the estimate from the g -tensor anisotropy obtained from the ESR spectrum. Thus, if one assumes the extreme values of the ESR signals as the parallel and perpendicular components of g , the maximum amount of anisotropy would be $\alpha = g_{\perp}^2/g_{\parallel}^2 \approx (0.2-0.3)$.

The unusual presence of ferromagnetic coupling in this complex deserves explanation. The fact that the Co-O-Co angles in the Co_4O_{16} group are 90° and $\sim 100^\circ$ suggests the possibility of an explanation based on orthogonality of the magnetic orbitals through the bridging oxygen atoms.²⁹

We note, however, that, in addition to superexchange pathways, several magnetic orbitals of cobalt atoms may have some degree of direct overlap owing to the geometry of the Co_4O_{16} group. A probably minor second source of the ferromagnetic exchange could therefore be related to the orbital degeneracy of the Co. In the framework of the Anderson model, this degeneracy could allow electronic transfers within the t_{2g} orbitals of two interacting Co atoms, keeping a parallel spin alignment on the virtual Co(I)-Co(III) excited state, that may provide a direct exchange pathway for the stabilization of the ferromagnetic state.

Work is underway in our laboratories on isostructural and similar complexes containing Cu(II), Ni(II), Co(II), Mn(II), and other transition metals which may clarify the points in the previous paragraph.

Calculational Methods

Exchange Hamiltonian. The general form of exchange Hamiltonian is shown^{30,31} by

$$H_{ex} = -2 \sum_{ij} J_{ij} S_i S_j \quad (2)$$

where J_{ij} represents the exchange between each pair of magnetic ions with spins S_i and S_j . In the present case the spin anisotropy of the Co atoms, numbered as in Figure 1, can be accounted for

(26) Simmons, V. E. Doctoral Dissertation, Boston University, 1963; *Diss. Abstr. Int.* 1963, 24, 1391.

(27) Mulay, L. N. In *Theory and Applications of Molecular Paramagnetism*; Boudreaux, E. A., Mulay, L. N., Eds.; John Wiley and Sons: New York, 1976; p 494.

(28) Coronado, E.; Drillon, M.; Nugteren, P. R.; de Jongh, L. J.; Beltran, D. *J. Am. Chem. Soc.* 1988, 110, 3907.

(29) Kahn, O. In *Magnetostructural Correlations in Exchange Coupled Systems*; Willett, R. D., Gatteschi, D., Kahn, O., Eds.; NATO ASI Series; Reidel: Dordrecht, Holland, 1985.

(30) Carlin, R. L. *Magnetochemistry*; Springer-Verlag: New York, 1983.

(31) Hatfield, W. E. In *Theory and Applications of Molecular Paramagnetism*; Boudreaux, E. A., Mulay, L. N., Eds.; John Wiley and Sons: New York, 1976; Chapter 7.

by an effective exchange anisotropy. Equation 2 can then be expressed as

$$H_{\text{ex}} = -2[J_z(S_{1z}S_{2z} + S_{2z}S_{3z} + S_{3z}S_{4z} + S_{4z}S_{1z} + S_{1z}S_{3z}) + 2J_{xy}[(S_{1x}S_{2x} + S_{2x}S_{3x} + S_{3x}S_{4x} + S_{4x}S_{1x} + S_{1x}S_{3x}) + (S_{1y}S_{2y} + S_{2y}S_{3y} + S_{3y}S_{4y} + S_{4y}S_{1y} + S_{1y}S_{3y})]] \quad (3)$$

Finally, taking into account the definition of scaling operators and defining the exchange anisotropy as $\alpha = J_{\perp}/J_{\parallel}$, the exchange Hamiltonian can be written

$$\hat{H}_{\text{ex}} = -2J_z[(\hat{S}_{1z}\hat{S}_{2z} + \hat{S}_{2z}\hat{S}_{3z} + \hat{S}_{3z}\hat{S}_{4z} + \hat{S}_{4z}\hat{S}_{1z} + \hat{S}_{1z}\hat{S}_{3z}) + \alpha[(\hat{S}_1^+\hat{S}_2^- + \hat{S}_1^-\hat{S}_2^+) + (\hat{S}_2^+\hat{S}_3^- + \hat{S}_2^-\hat{S}_3^+) + (\hat{S}_3^+\hat{S}_4^- + \hat{S}_3^-\hat{S}_4^+) + (\hat{S}_4^+\hat{S}_1^- + \hat{S}_4^-\hat{S}_1^+) + (\hat{S}_1^+\hat{S}_3^- + \hat{S}_1^-\hat{S}_3^+)]] \quad (4)$$

Zeeman Hamiltonian. The general form for a system containing four magnetic ions is

$$\hat{H}_{\text{Zeeman}} = -\sum_{i=1}^4 g_i \beta H S_i \quad (5)$$

Since two types of Co are present, two values of g are possible: $g_i = g_a$ for $i = 1, 3$ and $g_i = g_b$ for $i = 2, 4$. If an axial case is considered (consistent with the crystallographic data), two g components for each type of Co have to be taken: g_{\parallel} , g_{\perp} , g_{\parallel} , g_{\perp} . Then the Zeeman Hamiltonian may be split into components perpendicular and parallel to the magnetic field

$$\hat{H}_{\text{Zeeman}} = \hat{H}_{Z\parallel} + \hat{H}_{Z\perp} \quad (6)$$

where

$$\hat{H}_{Z\parallel} = -[g_{\parallel}(\hat{S}_{1z} + \hat{S}_{3z}) + g_{\parallel}(\hat{S}_{2z} + \hat{S}_{4z})]\beta H_Z \quad (7)$$

and

$$\hat{H}_{Z\perp} = -[g_{\perp}(\hat{S}_{1x} + \hat{S}_{3x}) + g_{\perp}(\hat{S}_{2x} - \hat{S}_{4x})]\beta H_x - [g_{\perp}((\hat{S}_1^+ + \hat{S}_1^-)/2 + (\hat{S}_3^+ + \hat{S}_3^-)/2) + g_{\perp}((\hat{S}_2^+ + \hat{S}_2^-)/2 + (\hat{S}_4^+ + \hat{S}_4^-)/2)]\beta H_x \quad (8)$$

since the x and y directions are equivalent.

Basis Functions. The spin wave functions for the Co_4 system can be written as products of the atomic spin functions

$$|S_1, S_{1z}\rangle |S_2, S_{2z}\rangle |S_3, S_{3z}\rangle |S_4, S_{4z}\rangle$$

abbreviated as $|S_{1z}, S_{2z}, S_{3z}, S_{4z}\rangle$. (The wave functions are given in the supplementary material.)

Since $S_i = 1/2$, the eigenvalue problem consists in solving a 16×16 matrix. Hence the energies corresponding to those states are obtained by solving the resulting determinant.

It is practical to separate the different contributions to the energy matrix into an exchange matrix and two Zeeman matrices (parallel and perpendicular). These matrices are given in the supplementary material.

Magnetic Susceptibilities. Knowledge of the eigenvalues, E_i , of the energy matrix allows one to calculate the molar magnetic susceptibilities from the expression

$$\chi_j = kT \left[\frac{\delta^2}{\delta H_j^2} \log \sum_i [\exp(-E_i(H_j)/kT)] H_j \right]_{H_j \rightarrow 0} \quad (9)$$

where j represents the components parallel or perpendicular to the magnetic field H . The (χ_{\parallel}) and (χ_{\perp}) are obtained from matrices derived from the parallel and perpendicular Zeeman Hamiltonians, respectively. The average molar susceptibility can be obtained by averaging them according to the formula

$$\chi_M = (\chi_{\parallel} + 2\chi_{\perp})/3 \quad (10)$$

As a result χ_M is expressed in terms of six parameters, J_{\parallel} , J_{\perp} , g_{\parallel} , g_{\perp} , g_{\parallel} , g_{\perp} , that can be refined as described below by a least-squares method to obtain the best fit.

The goodness of fit, F , is defined as the sum of the squares of the differences between observed and calculated susceptibilities relative to the observed values squared. The lower the F , the better the fit. As shown in Table II, various assumed values of α ($= J_{\perp}/J_{\parallel}$) lead to different F values and indicate that F is best when $\alpha \cong 0.3$. Then a further refinement in this vicinity was carried out wherein all parameters varied freely. This led to a best set of parameters, which are shown in the inset in Figure 2, which is a plot of experimental and calculated μ_{eff} versus T .

Observed and best-fit calculated χ_M values are given in Table I for T values less than 22 K. The best-fit calculated $1/\chi_M$ values are plotted as a solid line in Figure 3, along with the experimental values.

Acknowledgment. We are deeply grateful to Dr. Ekkehard Sinn for letting us use the SQUID magnetometer at the University of Virginia. N.C.-P. thanks the Spain-USA Joint Committee for Cultural and Educational Cooperation for a Fellowship. E.C. is grateful for a travel grant from the Generalitat Valenciana. E.C. and G.P. are grateful to Franco-Spanish Integrated Action.

Supplementary Material Available: Basis functions, Exchange matrix (16×16), and Zeeman matrices parallel and perpendicular to the field (5 pages). Ordering information is given on any current masthead page.